Effect of magnetic field structure on electron internal transport barrier and its role for the barrier formation in Heliotron J

T. Minami[1], N. Kenmochi[2], C. Takahashi[1], K. Nishioka[3], A. Ishizawa[4], G. Weir[5], Y. Nakamura[4], S. Kobayashi[1], H. Okada[1], S. Kado[1], S. Yamamoto[1], S. Ohshima[1], S. Konoshima[1], T. Mizuuchi[1] and K. Nagasaki[1]

[1]Institute of Advanced Energy, Kyoto University, Kyoto, Japan
[2]Graduate School of Frontier Sciences, The University of Tokyo, Chiba, Japan
[3]Theoretical Plasma Physics LaboratoryDepartment of Physics, Nagoya University, Japan
[4]Graduate School of Energy Science, Kyoto University, Kyoto, Japan
[5]Max-Planck-Institut für Plasmaphysik, Greifswald, Germany

Corresponding Author: minami@iae.kyoto-u.ac.jp

Abstract:

An effect of magnetic field configuration to form an electron internal transport barrier (eITB) and a role in forming the eITB in the helical plasma are discussed. In Heliotron J experiments, the eITB formation is determined not only by the neoclassical transport to produce the positive radial electric field but also by the existence of low-order rational surface. The low-order rational surface expands the improved confinement region generated by the eITB, and the power threshold to form the eITB for the plasma without the eITB is also reduced. Because a magnetic island can be formed on this rational surface, it is necessary to consider the effect of the magnetic island on the eITB formation.

1 Introduction

The electron internal transport barrier (eITB) can be formed in helical plasma (which is called by various names, high Te mode, hot electron mode, neoclassical internal transport barrier, or CERC [core electron-root confinement][1]). The eITB has been observed widely in helical devices such as CHS, LHD, TJ-II, and W7-AS, and it is also observed in Heliotron J[2, 3, 4, 5, 6, 7]. The improved confinement by the electron internal transport barrier (eITB) formation has been observed by electron cyclotron resonance heating (ECH) in low density plasma[8]. A transport analysis shows a clear reduction of effective thermal diffusivity in the core region[8]. One of the results of the Heliotron J experiments is the normalized threshold value of P_{ECH}/n_e for the eITB formation ($\sim 250 \times 10^{-19} kWm^3$)[8] is smaller than that of the other results of the helical plasma.

The eITB of the helical plasma can be explained by the generation of the positive radial electric field[1]. Due to the nonlinear dependence of the neoclassical transport particle fluxes on E_r in the helical plasma, E_r is determined by the ambipolar condition as follows:

$$\Gamma_e(E_r) = \Gamma_i(E_r) \tag{1}$$

, where Γ_i, Γ_e represents the particle flux of the plasma ions and electrons. Consequently, the positive radial electric field is produced by the electron-root solution of the ambipolarity condition of the neoclassical transport, which is caused by the helical ripple of the helical plasma.

Because the internal transport barrier has also been established by on-axis neutral beam injection heating with a reversed shear that was formed by a current ramp-up in JT-60U[9], thus the physical mechanism of the barrier formation is associated with the magnetic field configuration. Consequently, it is necessary to clarify the role of the magnetic field and magnetic field configuration to form the eITB for the helical plasma. The previous results of the experiments for the helical plasma, the importance of the low-order rational surface is pointed out. A low-order rational surface and a magnetic island can easily trigger the eITB formation[6] in TJ-II experiment. In the LHD experiments, the magnetic island located near the foot point of the eITB contributes to the formation of the eITB through the radial electric field shear production at the magnetic island boundary[5]. However, the detailed role of the rational surface and the magnetic island on the eITB formation is unclear yet.

In this paper, we discuss the role of magnetic field structure to form the eITB in helical plasmas. Section 2 shows a role of neoclassical transport through the helical ripple using bumpy component control of magnetic configuration. In Section 3, we discuss a role of the rational surface to expand an enhanced confinement region during the eITB formation. In Section 4, we discuss the role of the rational surface for the power threshold to form the eITB. Finally, we summarize the role of the magnetic configuration for the eITB formation.

2 Role of neoclassical transport through helical ripple

To clarify the role of the helical ripple to form the electron internal transport barrier is essential. A hypothesis on the physical mechanism by which the eITB is formed is that the barrier is easily formed in larger helical ripple (ϵ_{eff}) magnetic configuration, because the generation of the radial electric field depends on the magnetic field configuration through the neoclassical transport characteristics[1], in the helical plasma, which is mainly determined by the helical ripple. The previous CHS results show that the eITB of the magnetic configuration that has the larger ϵ_{eff} ($R_{ax} = 94.9cm$) has higher electron pressure in the enhanced confinement region compared to that with smaller ϵ_{eff} (Rax=92.1cm), although the confinement without the transport barrier of the small ϵ_{eff} configuration is better than that of the larger ϵ_{eff} configuration[4]. The estimated neoclassical radial electric field of

the larger ϵ_{eff} configuration is also larger than that of the smaller one. Therefore, the larger helical ripple configuration can produce the larger radial electric field and the larger confinement improvement.

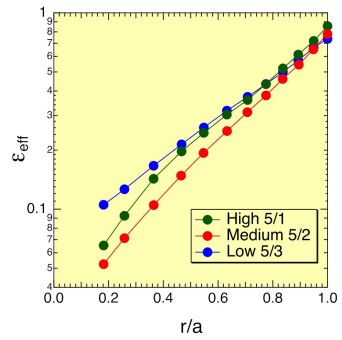

FIG. 1: The ϵ_{eff} profile of for high (5/1), medium (5/2) and low (5/3) configurations in Heliotron J.

The effect of the ripple on the eITB formation was investigated to confirm the hypothesis in Heliotron J, the. A bumpy component of the magnetic configuration can be controlled by two sets of eight toroidal field coils with different coil currents (I_{TA}, I_{TB})[11]. The neoclassical transport of the helical plasma is characterized by the effective helical ripple (ϵ_{eff}), which characterize the helical $1/\nu$ electron transport[12]. The ϵ_{eff} is defined by the following equation.

$$\epsilon_{eff} = \left[\frac{9\sqrt{2}\pi}{16}\frac{\nu}{\nu_d^2}D\right]^{2/3} \quad (2)$$

, where ν, ν_d and D are the collision frequency, the drift velocity and particle the diffusion coefficient, respectively.

The ϵ_{eff} of for three types of the magnetic configurations, high $(I_{TA}/I_{TB} = 5/1)$, medium $(I_{TA}/I_{TB} = 5/2)$ and low $(I_{TA}/I_{TB} = 5/3)$ bumpiness configurations in Heliotron J are calculated[13]. The results (Fig.1) show that the high and low bumpiness configurations have the higher ϵ_{eff} compared to the medium bumpiness configuration in the core region $(r/a < 0.5)$, in which the eITB easily can be formed.

The Heliotron J is a medium-sized device with a periodicity of (l, m) = (1,4). The major and averaged minor radii are 1.2 and $0.1 - 0.2m$, respectively[14]. The magnetic field strength is $1.25T$, and the working gas is deuterium. The plasma with eITB is produced by a centrally focused $70GHz$ ECH ($P_{inj} \sim 250kW$, $N_{||} = 0.0$). The electron temperature and density are measured with Nd:YAG Thomson scattering system.

Figure 2 shows the electron temperature of the ECH plasma as a function of the injected power divided by the line averaged density in low density region $(n_e < 1 \times 10^{19}m^{-3})$. The electron temperature is increased by the eITB formation through the transport improvement, and its gradient also increases at the location of the barrier formation. As shown in Fig.2, the power thresholds to form the eITB in the low and the high bumpiness configurations are larger $(P_{ECH}/n_e \sim 550 \times 10^{-19}kWm^3)$ than that of the medium bumpiness $(\sim 250 \times 10^{-19}kWm^3)$. Consequently, the smaller ϵ_{eff} configuration has the lower power threshold in Heliotron J, and this result does not agree with the CHS results and the hypothesis. Although the results may relate to the small difference of ϵ_{eff}f in Heliotron J compared to that of CHS, the large drop of the threshold value in the medium bumpiness

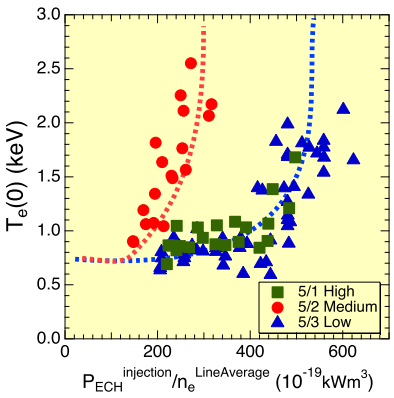

FIG. 2: Central electron temperature of ECH plasma as a function of injected power divided by line averaged density.

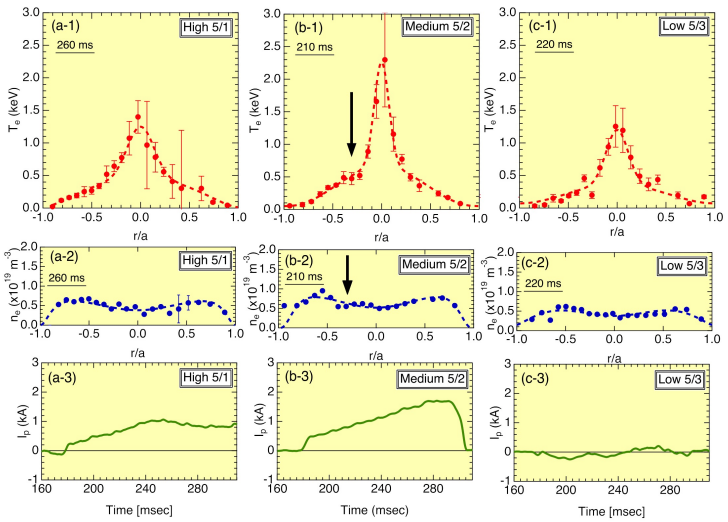

FIG. 3: Electron density and temperature profiles for low, medium and high bumpiness magnetic configurations.

configuration shows that the eITB formation is not determined by ϵ_{eff} alone.

Figure 3 shows the electron density and temperature profiles for the three different magnetic configurations, and time evolution of the plasma currents are also shown. Although the difference of the density profiles is small, the electron temperature profile of the medium bumpiness profile is steeper and narrower than that of the high and low bumpiness configurations. The flattening of the temperature and density profile shapes are observed around $r/a \sim -0.3$, where O-point of the magnetic island ($n/m = 4/7$) is expected to be formed in Heliotron J (location of $r/a \sim 0.3$ is X-point of the island). The $n/m = 4/7$ rational surface is critical because the surface is a candidate where the magnetic island is produced due to the n=4 toroidal periodicity of the vacuum magnetic field of Heliotron. The magnetic island can be formed on the 4/7 low-order rational surface by the small plasma current, because the vacuum iota values of the three magnetic configurations are close 4/7 rational surface. The medium bumpiness configuration has large plasma current compared to the high bumpiness configuration, and the plasma current of low bumpiness is very small. These results have an agreement with the previous boot-strap current experiment in Heliotron J[15]. Consequently, the 4/7 rational surface or the magnetic island may be formed in the medium bumpiness configuration. Therefore, we can provide the second hypothesis that there is a possibility that the rational surface or the magnetic island affects the eITB formation.

3 Role of the rational surface to expand improved confinement region

We investigate an effect of a low-order rational surface on the improved confinement region (eITB foot point) to confirm the second hypothesis in Heliotron J. The magnetic shear of the rotational transform of Heliotron J is considerably small compared to that of CHS, and the rational surfaces easily appear with the small plasma current of the order of kA

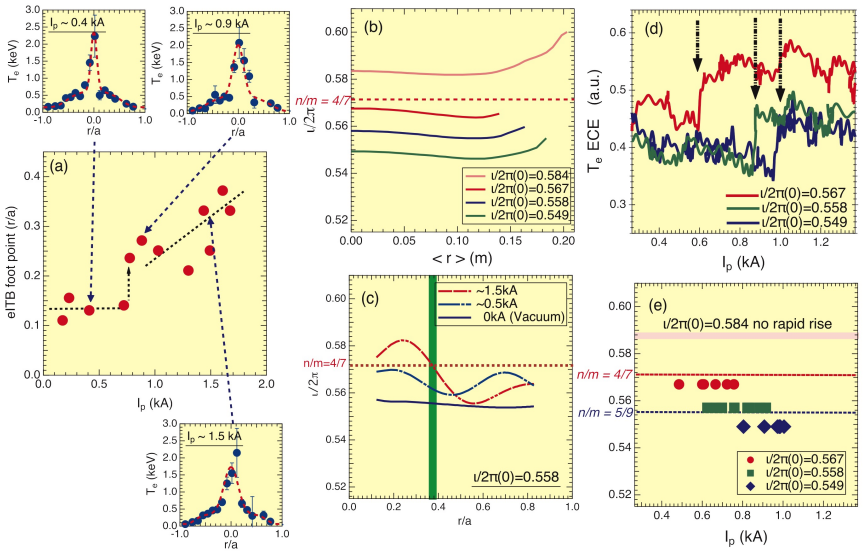

FIG. 4: (a) eITB foot point as a function of plasma current. (b)$\iota/2\pi$ profiles (c)$\iota/2\pi$ profile of 0.558 with bootstrap current. (d) ECE signals as a function of plasma current. (e) Plasma current when the rapid temperature jump occur.

on the shearless configuration. We have investigated the effect of the magnetic topology on the eITB formation in Heliotron J.

The experiments have been performed on the medium bumpiness magnetic configuration of $B_{ax} = 1.25T$. The vacuum rotational transform profile is almost flat and the value of central ι is 0.558 4(b)). The plasma with eITB is also produced by a centrally focused $70GHz$ ECH ($P_{inj} \sim 270kW$, absorption ratio is above $\sim 90\%$). The power threshold $(P_{injection}/n_e)$ is controlled to form eITB from the beginning of the plasma discharge by gas-puffing. The plasma current that is mainly driven by bootstrap gradually ramps up to $1.5kA$ and the ration of the ECH driven current is small due to $N_{||} = 0.0$. The eITB footpoints are plotted as a function of the plasma current, as shown in4(a). When the plasma current increases up to $0.7kA$, the barrier location stay almost the same location as $r/a \sim 0.13$. When the current increases up to $\sim 0.7kA$, the location of the barrier foot point rapidly moves towards outside of the plasma from $r/a \sim 0.13$ to 0.25. After that, the barrier further moves to the outside and reaches the location of $r/a \sim 0.35$ although the central temperature slightly decreases as the expansion of the improved region.

The estimation of the bootstrap current profile that is calculated by the DKES code with the Sugama-Nishimura method[16] is shown in 4(c). The calculation is carried out using the profiles that are measured with Nd:YAG Thomson system. The rotational transform profile including bootstrap current is calculated by VMEC code[17]. The calculation shows that the bootstrap current is driven in the plasma core by the steep temperature gradient, which is formed by the barrier formation. When the plasma current is higher than the value of $\sim 0.5kA$, the 4/7 rational surface is formed. It moves to the outside of the plasma with the increase of the bootstrap current. The calculated location of the 4/7 rational surface has accordance with the location of the eITB foot point.

The eITB formation for the different rotational transform values of $\iota(0) = 0.549, 0.567$

and 0.584 has been also investigated. The profiles of the rotational transform are shown in 4(b). The plasma with eITB is also produced by a centrally focused $70GHz$ ECH ($P_{inj} \sim 270kW$). The plasma density is controlled to be fixed by a gas-puffing because the condition of the eITB formation depends on the plasma density. Figure 4(d) shows the ECE signals as the function of the plasma current for three different rotational transform plasmas. The plasma current value when the rapid increase of the electron temperature occurs is delayed by reducing the rotational transform values. In addition, no rapid increase has been observed for the magnetic configuration of $\iota(0) = 0.584$. Because the bootstrap current is driven to the direction of the rotational transform increase, the 4/7 rational surface cannot be produced in the $\iota(0) = 0.584$. Figure 4(e) shows that the current value at which the rapid increase of the ECE signal occurs for the different vacuum ι plasmas. The required plasma current to the confinement region expansion decreases with the decrease of the rotational transform values except for the rotational profile of $\iota(0) = 0.584$.

The other low-order rational surfaces (ex. $n/m = 5/9 \sim 0.556$) on which the magnetic island is not formed have no relation with the phenomena. Therefore, these observations suggest the possibility that the phenomena relate to the magnetic island formations. In summary, the eITB can be formed without the low-order rational surface or the magnetic island, they affect the barrier location and enhance the confinement.

The similar mechanism that the magnetic island affects the plasma transport has also been observed in numerical simulation. In Ref. [18], the simulation shows that transport is reduced in the core plasma region adjacent to the magnetic island by the micro-turbulence reduction, which is caused by the flow shear increase around the magnetic island.

4 Role of the rational surface for the power threshold to form the eITB

It is important to investigate an effect of the low-order rational surface on the power threshold to form the eITB. In this experiment, the magnetic configuration is the medium bumpiness configuration of $\iota(0) = 0.558$. The plasma with eITB is also produced by the $70GHz$ ECH, of which injected power is constant ($P_{inj} \sim 250kW$). The plasma is produced by off-axis heating (resonance zone: $r/a \sim 0.1$) to disappear the eITB at the beginning of the discharge because the off-axis heating is unfavorable to form eITB[4]. The plasma density was adjusted to be almost constant ($\bar{n}_e \sim 1 \times 10^{19} m^{-3}$) by the the gas-puffing, as shown in Fig.5. Consequently, the plasma is sustained to be close to the limit power threshold not to form the eITB. The plasma current is

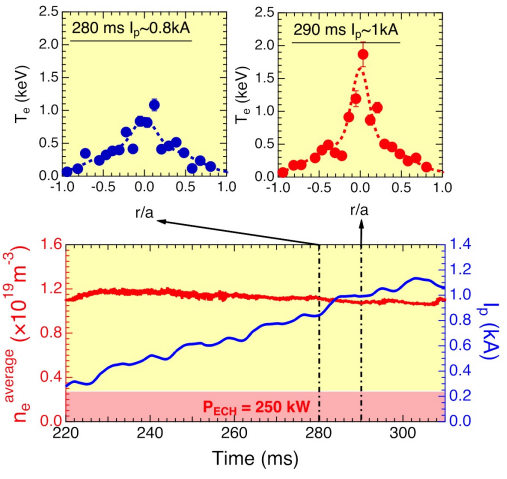

FIG. 5: Electron temperature profiles before and after plasma current of $\sim 0.9kA$ with temporal evolution of electron density and current.

also mainly driven by the bootstrap current due to $N_{||} = 0.0$, and gradually increases during the discharge, as shown in Fig.5. The 4/7 low-order rational surface is expected to be created by the current ramp up. Figure 5 shows the electron temperature profiles before and after the current value reaching $\sim 0.9kA$. Although the electron temperature profiles are almost same before reaching $\sim 0.9kA$, the temperature of the plasma core increases after reaching the value of $\sim 0.9kA$ compared to that before reaching, of which characteristic shows the eITB formation.

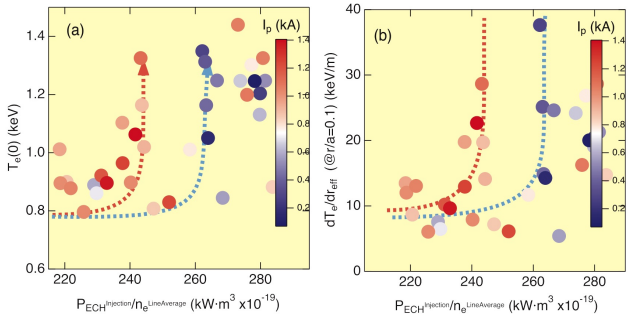

FIG. 6: Central electron temperatures and gradients on the barrier location are plotted as a function fo the injected power over the averaged density.

The same experiments as above mentioned are carried out for plasmas of different densities ($n_e \sim 0.7-1.2\times 10^{19}m^{-3}$) to clarify the effect of the rational surface for the power threshold. The central electron temperatures and gradients on the barrier location are plotted as a function of the injected power over the averaged density, as shown in Fig.6. The color of the makers show the plasma current values. The increase of the temperature and the gradient are caused by the barrier formation. These results clearly show that the power threshold reduction to form the eITB from $265kWm^3$ to $240kWm^3$ when the plasma current increases above $I_p \sim 0.9kA$. The plasma current of $0.9kA$ is almost the same as the calculated value that is required to form 4/7 rational surface. Because the two thresholds above and below $0.9kA$ are separated, it can be explained that the threshold reduction has occurred due to the formation of the 4/7 rational surface.

The plasma current increase does not directly relate to the eITB formation. The electron temperatures and the gradients as a function of the plasma currents are plotted in Fig.7. The graphs show that there are no relations between the plasma current and the barrier formation. Therefore, the eITB cannot be formed only by the existence of the rational surface, and the eITB formation by the current increase as is shown in Fig.6 can be explained by the reduction of the threshold.

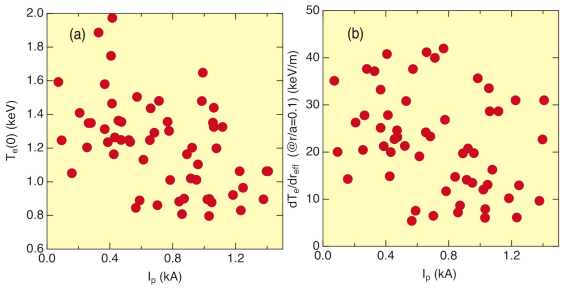

FIG. 7: Electron temperatures and the gradients as a function of the plasma currents.

5 Summary

The eITB formation is determined not only by the neoclassical transport through the helical ripple but also by the existence of low-order rational surface. Although The eITB

of the helical plasma can be formed without the low-order rational surface, the existence of the low-order rational surface brings favorable effects on the eITB formation. The rational surface can expand the improved confinement region, and the power threshold for the eITB formation decreases due to the existence of the rational surface. It is necessary to take account of the effect of not only neoclassical transport but also the magnetic island on the eITB formation.

Acknowledgment

This work was supported by the NIFS collaborative Research Program (NIFS17KUHL074, NIFS16KUHL07, NIFS17KUHL07, NIFS18KUHL083, NIFS18KUHL085, NIFS18KUHL088, and NIFS10KUHL030). We deeply appreciate Prof. Shoichi Okamura for the calculation of the effective helical ripple.

References

[1] YOKOYAMA, M., et al., Nucl. Fusion, **47**, 1213-1219 (2007)

[2] FUJISAWA, A., et al., Phys. Rev. Lett., **82** (13) 2669 (1999)

[3] MINAMI, T., et al., Nucl. Fusion, **44** 342 (2004)

[4] MINAMI, T., et al., Plasma Phys. Control. Fusion **46** A285-A290 (2004)

[5] IDA, K., et al Phys. Plasmas **11** No.5 (2004)

[6] CASTEJO'N F., et al., Nucl. Fusion, **44** (2004)

[7] MAAßBERG H., et al., Phys. of Plasmas **7** No.1 295 (2000)

[8] KENMOCHI. N., et al., Plasma Phys. Control. Fusion 59 (2017) 055013

[9] FUJITA, T., et al 1998 Nucl. Fusion 38 207

[10] OKAMURA, S., et al., Nucl. Fusion, **39**, No. 9 (1999)

[11] WAKATANI, M., et al., Nucl. Fusion, **40** No.3 569 (2000)

[12] BEIDLER, D. C., et al., Plasma Phys. Control. Fusion, **36** 317 (1994)

[13] HEYN, F. M., et al., Plasma Phys. Control. Fusion, **43** 1311 (2001)

[14] OBIKI, T et al., Nucl. Fusion, **41**, No. 7 833 (2001)

[15] MOTOJIMA.G, et al.,Fusion Sci. Technol. 51, 122 (2007).

[16] SUGAMA, H and NISHIMURA, S, Phys. Plasmas 9, 4637 (2002)

[17] HIRSHMAN, S.P.. J. WHITSON, C., Phys. Fluids 26, 3553(1983)

[18] ISHIZAWA, A., NAKAJIMA, N., Nucl. Fusion 49 (2009) 055015 (9pp)